4B.6 AGGREGATE-AREA RADIATIVE FLUX BIAS CORRECTIONS OVER SEA ICE

Xuanji Wang[1*] and Jeffrey R. Key[2]
[1]Cooperative Institute for Meteorological Satellite Studies, University of Wisconsin-Madison, Madison, Wisconsin
[2]Office of Research and Applications, National Environmental Satellite, Data, and Information Service, NOAA
Madison, Wisconsin

1. INTRODUCTION

Sea ice and climate models have relatively coarse grids, typically on the order of 100-250 km. In the computation of radiation fluxes, surface and atmospheric properties are treated as being horizontally homogeneous and average grid cell properties are used, either with radiative transfer models or simple paramerization schemes. Recent studies have shown that this assumption can result in errors in estimating surface radiation and turbulent fluxes because some atmospheric and surface properties are nonlinear with respect to surface radiation fluxes (Marshak, 1995; Liou, 1979; Mahrt, 1987; Sellers, 1991; Friedl, 1996).

The purposes of this paper are to (a) assess the degree of spatial-temporal variability in the surface, cloud, and radiative parameters over sea ice using satellite data, (b) evaluate the biases in radiative fluxes calculated from area average surface and cloud properties versus averages of fluxes calculated at a relatively high spatial resolution, and (c) develop a simple regression approach to correcting the biases.

2. FORMULATION, DATA AND METHODS

Grid cell radiative fluxes are computed in two ways: calculate the fluxes with average surface and cloud properties over a grid cell, analogous to what is done in models, and calculate flux for every 5x5 km^2 satellite pixel within the hypothetical grid cell, then average those fluxes over the cell. We refer the former method as the *area-average* method, and the latter as the *pixel-average* method which is similar to the concept of the “independent pixel approximation” used in studies of three-dimensional radiative transfer effects (cf., Marshak et al., 1998).

Semivariance analysis is employed to describe the spatial and temporal variability of the surface radiative fluxes, cloud, and surface properties. The semivariogram is a structure function that, like autocorrelation, describes the correspondence between observations made at some distance or time lag. Therefore, a parameter measured at one location or time provides some information about the parameter at other locations or times. The semivariance *r(h)* for a distance lag h is defined as:

$$r(h) = \frac{1}{2N}\sum_{i=1}^{N}[\phi(x_i) - \phi(x_i + h)]^2 \qquad (1)$$

where *x* is a location, *N* is number of data points and ϕ describes the data, e.g., albedo or temperature. The change in semivariance with lag illustrates how rapidly the autocorrelation changes, while the magnitude of the semivariance indicates the degree of variability.

Data from the Advanced Very High Resolution Radiometer (AVHRR), on-board NOAA polar-orbiting satellites, are used in this study. The specific data set is a product of the AVHRR Polar Pathfinder (APP) project (Meier et al., 1997; Maslanik et al., 1998; Maslanik et al., 1999; Maslanik et al., 2000). The APP data are twice-daily composites available at 5x5 km^2 pixel size for June 1981-1998. The study period (September 1997 - August 1998) and the area correspond to the Surface Heat Budget of the Arctic Ocean (SHEBA) field experiment, where an icebreaker drifted with the pack ice for one year (Moritz et al., 1993).

We have extended APP standard products to include the all sky surface skin temperature, broadband albedo, cloud properties (particle phase, effective radius, optical depth, temperature, and pressure), and radiative fluxes using algorithms in the Cloud and Surface Parameter Retrieval (CASPR) system (Key, 2000). Downwelling radiative fluxes are computed in CASPR using *FluxNet* (Key and Schweiger, 1998). See Key (2000) and references therein for more information on the algorithms and their validation.

3. SPATIAL AND TEMPORAL VARIABILITY

Figure 1 shows a time series of AVHRR retrievals for downwelling shortwave and longwave fluxes at the surface (denoted as SWD and LWD, respectively), cloud optical depth (TAU), and surface temperature around the SHEBA ship site. The results shown are averages over a 55 x 55 km^2 area centered on the ship and smoothed with a 5-day running mean filter. The temporal persistence of downwelling shortwave and longwave fluxes, net radiation flux (NET), cloud fraction, cloud optical depth, surface broadband albedo, surface skin temperature is illustrated as a semivariogram in Figure 2. The semivariance of each parameter was normalized by the maximum semivariance.

---

[*] *Corresponding author address: Xuanji Wang, AOS, University of Wisconsin-Madison, 1225 West Dayton Street, Madison, WI 53706;*
email: xuanjiw@ssec.wisc.edu.

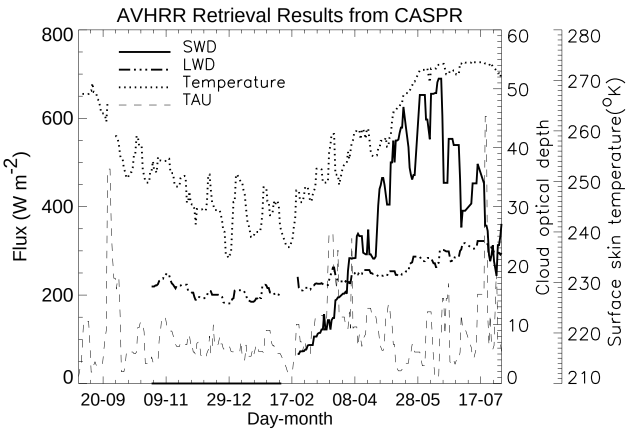

Figure 1. Time series of downwelling shortwave (SWD) and longwave (LWD) fluxes at the surface, cloud optical depth (TAU) and surface temperature. Values are averages over an area of 55 x 55 km^2 centered on the SHEBA ship and smoothed with a 5-day running mean.

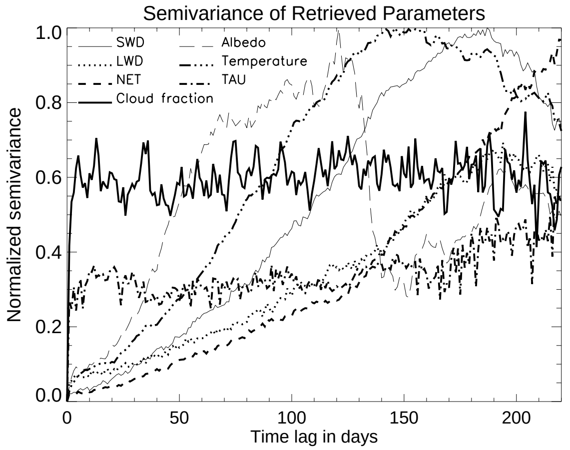

Figure 2. Time lag semivariogram for surface downwelling shortwave and longwave (SWD and LWD) fluxes, cloud optical depth (TAU), cloud fraction, surface broadband albedo, surface skin temperature and net radiation at the surface. The semivariance of each parameter was normalized by the maximum semivariance.

For both downwelling shortwave and longwave fluxes the maximum variance (the “sill”) is reached after 180 days, implying strong temporal correlations. But for cloud fraction and cloud optical depth the persistence is weak, indicating that there is almost no temporal correlation. Another interesting feature is that the net radiation flux at the surface has a different range than that of downwelling shortwave and longwave fluxes, reaching the sill about after 220 days. Figure 3 shows the spatial semivariogram of surface and cloud properties for June 1998, based on monthly mean values along the longitude 165^{o}W. Cloud fraction is not shown because subpixel cloud fraction was not computed. As with the temporal semivariogram, radiative fluxes, surface skin temperature, and surface broadband albedo show persistence with distance. Cloud particle effective radius and optical depth do not, indicating that clouds in this area and time are not horizontally homogeneous as is commonly assumed in sea ice and climate models. The gradual increase in the normalized semivariance of surface skin temperature and broadband albedo relative to that of cloud optical depth and shortwave radiation implies that the spatial variance increases much less rapidly for surface properties than for cloud properties. An interesting feature of downwelling fluxes and surface albedo is that the semivariogram shows sinusoidal wave patterns with spatial scale. Cloud optical depth also shows a similar wave pattern with spatial scale. This phenomenon may be related to synoptic scale weather systems, at least in June over this portion of the Arctic. It clearly shows that most parameters change with spatial scale in a non-linear way.

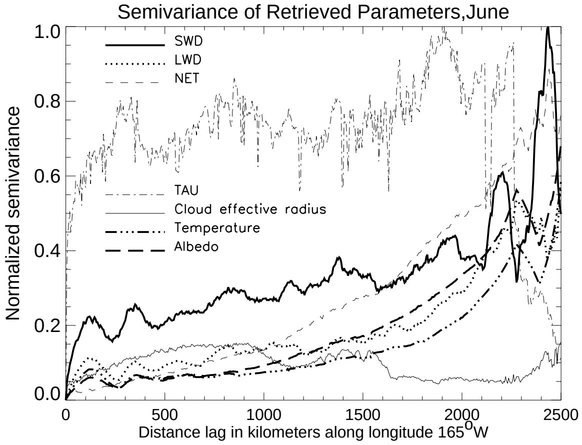

Figure 3. Space lag semivariogram for surface downwelling shortwave and longwave (SWD and LWD) fluxes, cloud optical depth (TAU), cloud fraction, surface albedo, surface temperature, cloud effective radius, and net radiation flux at the surface. The semivariance of each parameter was normalized by the maximum semivariance. Monthly means along longitude 165^{o}W were used.

4. FLUX CALCULATION AND BIAS CORRECTION

We expect that the fluxes calculated with these two methods will be different because (a) surface and cloud parameters exhibit spatial variability on scales less than that of a typical climate or ice model grid cell, (b) the magnitude of the variability differs for each parameter, and (c) the relationship between some parameters and surface radiation is non-linear. To test that hypothesis, both methods were used to compute the flux biases in the downwelling shortwave (SWD) and longwave (LWD) radiative flux calculations, where the bias is defined as the area-average flux minus the pixel-average flux. Figure 4. shows the percentage biases of downwelling shortwave and longwave fluxes regarding to the pixel-average fluxes. The bias can be as large as 22% for both of downwelling shortwave and longwave fluxes, indicating the correction should be taken into account when parameterization is used to calculate the model grid cell fluxes, and results also indicate that the flux biases are nearly scale invariant, especially for the downwelling longwave radiative flux in our 14 hypothetical model grid cell sizes (from 15x15 km^2 to 505x505 km^2).

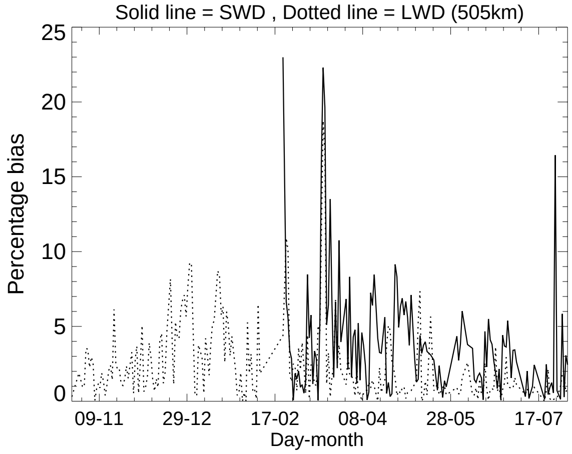

Figure 4. The percentage bias of downwelling shortwave (SWD) and longwave (LWD) fluxes regarding to the pixel-average fluxes. The bias defined as area-average flux minus pixel-average flux, therefore the percentage bias is equal to bias divided by the pixel-average flux. The solid line is SWD, and dotted line is LWD for area size of 505 x 505 km^2. For other area sizes the figure and the percentage bias are very similar to this one.

An analysis of the relationship between the biases and parameters were performed by using multivariate regression analysis (Liou, 1979). Examinations of all surface and cloud properties revealed that combinations of cloud fraction (C), cloud optical depth (τ), surface broadband albedo (α) and solar zenith angle (μ) for SWD flux biases influence the magnitude of the biases to a much greater degree than other parameters. For the LWD flux biases the cloud fraction, surface skin temperature (T) and their combination contribute the most to the explanation of bias variance. For SWD fluxes the biases tend to change from negative to positive when the cloud optical depth becomes larger. When the cloud fraction is small and/or surface skin temperature is low, the LWD flux biases are negative, with the increases of the cloud fraction and/or temperature the LWD biases change to positive. By multiple correlation analysis, the five parameters used to estimate the SWD flux biases are cloud fraction, cloud optical depth, cloud fraction times cloud optical depth, cloud fraction times cloud optical depth and cosine of solar zenith angle and surface broadband albedo. The multiple correlation coefficient for five parameters used to estimate SWD flux biases is 0.63. For the LWD flux biases three parameters were adopted to do the bias estimates, which are cloud fraction, surface skin temperature and cloud fraction times surface skin temperature, and the multiple correlation coefficient is 0.62.

The regression analysis was performed on the SHEBA AVHRR retrievals. Regression equations were developed to estimate the SWD and LWD flux biases, but with only those terms that passed the statistical significance test (at a significance level of 0.05.) remain in the regression equations. The regression equations are:

$$\mathrm{SWDBias} = -5.6519 + 0.33793\tau + 18.246C - 3.9539C\tau + 3.3107C\tau\mu + 2.1057C\tau\alpha \qquad (3)$$

$$\mathrm{LWDBias} = -77.403 + 73.115C + 0.28325T - 0.26119CT \qquad (4)$$

Figures 5 and 6 show the uncorrected and corrected bias frequency distributions. The bias correction equations are applicable to all model grid cells tested (from 15 x 15 km^2 to 505x505 km^2).

5. CONCLUSION

Satellite retrievals of surface, cloud, and radiation parameters over sea ice were used to investigate the spatial and temporal variability of surface and atmospheric parameters in the western Arctic during the SHEBA experiment. Downwelling shortwave and longwave fluxes at the surface exhibit temporal correlation over a long time period (about 180 days), but cloud optical depth and cloud fraction have nearly no correlation over the time period. Radiative fluxes, surface skin temperature, and surface broadband albedo also show persistence with distance, while cloud particle effective radius and optical depth do not. The spatial variance increases much less rapidly for surface properties than for cloud properties. A simple regression approach to correcting the fluxes for biases that result from horizontal variability was developed by computing average radiative fluxes as (a) the mean of fluxes calculated for every 5x5 km^2 pixel, and (b) the result of using area average mean surface and cloud properties in the flux calculation. The correction was found to reduce the average bias to nearly zero. The correction can be easily implemented in numerical models.

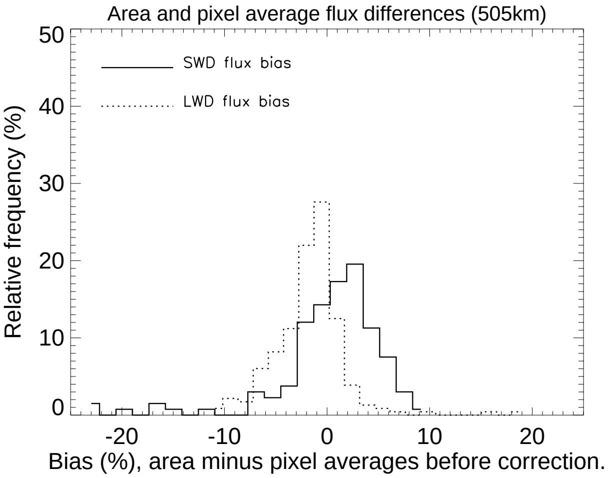

Figure 5. Relative frequency of flux differences for the area average and pixel average flux computations before correction. Values shown are for the period September 1997 through August 1998. Downwelling shortwave and longwave radiation fluxes are denoted by SWD and LWD, respectively.

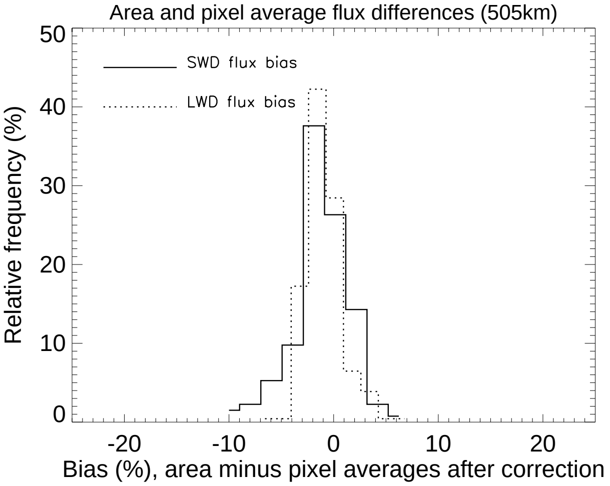

Figure 6. Relative frequency of flux differences for the area average and pixel average flux computations after correction. Values shown are for the period September 1997 through August 1998. Downwelling shortwave and longwave radiation fluxes are denoted by SWD and LWD, respectively.

ACKNOWLEDGMENTS

This research was supported by NASA grants NAG5-8625 and NAG5-6666, and NSF grant OPP-0096085. We thank C. Fowler, J. Maslanik, T. Scambos, and T. Haran for all their work on the AVHRR Polar Pathfinder data set.

REFERENCES

Friedl, M.A., 1996. Relationships among remotely sensed data, surface energy balance, and area-averaged fluxes over partially vegetated land surfaces. *J. App. Meteor.,* **35**(11), 2091-2103.

Key, J., 2000. The cloud and surface parameter retrieval (CASPR) system for polar AVHRR. Cooperative Institute for Meteorological Satellite Studies, University of Wisconsin, Madison, 59 pp.

Key, J. and A.J. Schweiger, 1998. Tools for atmospheric radiative transfer: Streamer and FluxNet. *Computers and Geosciences*, **24**(5), 443-451.

Liou, K. and G.D. Wittman, 1979. Parameterization of the radiative properties of clouds. *J. Atmos. Sci.*, **36**, 1261-1273.

Mahrt, L., 1987. Grid-Averaged surface fluxes. *Mon. Wea. Rev*., **115**(8), 1550-1560.

Marshak, A., A. Davis, R.F. Cahalan, and W. Wiscombe, 1998. Nonlocal independent pixel approximation: Direct and inverse problems. *IEEE Trans. Geosci. Remote Sens*., **36**(1), 192-205.

Marshak, A., A. Davis, R.F. Cahalan, W. Wiscombe and R. Cahalan, 1995. Radiative smoothing in fractal clouds. *J. Geophys. Res*., **100**(D12), 26247-26261.

Maslanik, J.A. and R.A. Silcox, 1993. Temporal variation of cloud fraction: Effects on a simulated sea-ice cover. *Geophys. Res. Lett*., **20**(23), 2651-2654.

Maslanik, J., C. Fowler, J. Key, T. Scambos, T. Hutchinson, and W. Emery, 1998. AVHRR-based polar pathfinder products for modeling applications. *Annals of Glaciol.*, **25**, 388-392.

Maslanik, J.A., A. Lynch, and C. Fowler, 1999. Assessing 2-D and coupled-model simulations of sea ice anomalies using remotely-sensed polar pathfinder products. *Proceedings of the Fifth Conference on Polar Meteorology and Oceanography*, American Meteorological Society, Dallas, TX, 10-15 January, 476-479.

Maslanik, J.A., J. Key, C.W. Fowler, T. Nguyen, and X. Wang. 2000. Spatial and temporal variability of satellite-derived cloud and surface characteristics during FIRE-ACE. *J. Geophys. Res*. (in press).

Meier, W.N.,J.A. Maslanik, J.R. Key, and C.W. Fowler, 1997. Multiparameter AVHRR derived products for Arctic climate studies. *Earth Interactions*, **1**, paper no. 5 (electronic journal only).

Moritz, R.E., J.A. Curry, N. Untersteiner, and A.S. Thorndike, 1993. Prospectus: Surface heat budget of the Arctic Ocean. NFSF-ARCSS OAII Tech. Rep. 3, 33 pp. Available from the SHEBA Project Office, Polar Science Center, Applied Physics Laboratory, University of Washington, Seattle, WA 98105.

Sellers, P., 1991. Modeling and observing land-surface-atmosphere interactions on large scales. *Surv. Geophys.*, **21**(1), 85-114.

Wang, X. and J.R. Key, 2001. Spatial Variability of the Sea Ice Radiation Budget and its Effect on Aggregate-Area Fluxes. *Annals of Glaciology*, (in press).